Developmental Cell
Article

Drosophila rasiRNA Pathway Mutations Disrupt Embryonic Axis Specification through Activation of an ATR/Chk2 DNA Damage Response

Carla Klattenhoff,[1] Diana P. Bratu,[1,3] Nadine McGinnis-Schultz,[1] Birgit S. Koppetsch,[1] Heather A. Cook,[2] and William E. Theurkauf[1,*]
[1] Program in Molecular Medicine and Program in Cell Dynamics, University of Massachusetts Medical School, Worcester, MA 01605, USA
[2] Department of Biological Sciences, Wagner College, Staten Island, NY 10301, USA
[3] Present address: Department of Biological Sciences, Hunter College, New York, NY 10021, USA
*Correspondence: william.theurkauf@umassmed.edu
DOI 10.1016/j.devcel.2006.12.001

SUMMARY

Small repeat-associated siRNAs (rasiRNAs) mediate silencing of retrotransposons and the *Stellate* locus. Mutations in the *Drosophila* rasiRNA pathway genes *armitage* and *aubergine* disrupt embryonic axis specification, triggering defects in microtubule polarization as well as asymmetric localization of mRNA and protein determinants in the developing oocyte. Mutations in the ATR/Chk2 DNA damage signal transduction pathway dramatically suppress these axis specification defects, but do not restore retrotransposon or *Stellate* silencing. Furthermore, rasiRNA pathway mutations lead to germline-specific accumulation of γ-H2Av foci characteristic of DNA damage. We conclude that rasiRNA-based gene silencing is not required for axis specification, and that the critical developmental function for this pathway is to suppress DNA damage signaling in the germline.

INTRODUCTION

RNA interference (RNAi) and related processes utilize short RNAs to direct protein complexes to chromatin and RNA, triggering heterochromatin formation, transcriptional silencing, translational repression, or RNA destruction (Hannon, 2002; Hutvagner and Zamore, 2002; Wassenegger, 2005). Mutations that disrupt small RNA functions affect a remarkable range of processes, including early embryogenesis in mice (Bernstein et al., 2003), embryonic morphogenesis in zebrafish (Giraldez et al., 2005), chromosome segregation in cultured chicken cells (Fukagawa et al., 2004) and yeast (Provost et al., 2002; Volpe et al., 2003), and developmental timing in worms (Grishok et al., 2001). In *Drosophila*, RNAi-related functions are required for stem cell division, stem cell maintenance, and viral immunity (Forstemann et al., 2005; Hatfield et al., 2005; Galiana-Arnoux et al., 2006; Wang et al., 2006). However, the full scope of biological functions controlled by small RNAs is only beginning to emerge, and the targets for most small RNAs have not been identified.

Mutations in the *Drosophila armitage* (*armi*), *spindle-E* (*spn-E*), and *aubergine* (*aub*) genes disrupt siRNA-guided RNA cleavage and assembly of the RNA-induced silencing complex (RISC) in ovary extracts and the production of 24–30 nt repeat-associated siRNAs (rasiRNAs), which are linked to retrotransposon and *Stellate* locus silencing (Aravin et al., 2004; Tomari et al., 2004a; Vagin et al., 2006). Strong loss-of-function mutations in these genes disrupt embryonic axis specification, triggering defects in microtubule organization and microtubule-dependent localization of mRNA and protein determinants in the developing oocyte (Cook et al., 2004). By contrast, mutations in *argonaute-2* (*ago-2*) and *dicer-2* (*dcr-2*) that disrupt the siRNA pathway, but do not block rasiRNA production, are viable and fertile (Deshpande et al., 2005; Lee et al., 2004; Okamura et al., 2004; Tomari et al., 2004b; Vagin et al., 2006). The rasiRNA pathway thus appears to have an essential function in embryonic axis specification; however, the critical developmental targets for this pathway have not been defined.

Mutations in the *armi*, *aub*, and *spn-E* genes lead to premature expression of Oskar (Osk) protein during early oogenesis (Cook et al., 2004), suggesting that overexpression of axis specification genes could lead to the patterning defects associated with rasiRNA pathway defects. However, here we show that the axis specification defects associated with *armi* and *aub* are dramatically suppressed by null mutations in *mei-41* and *mnk*, which respectively encode ATR and Chk2 kinases that function in DNA double-strand break (DSB) signaling. We also show that rasiRNA pathway mutations lead to germline-specific accumulation of γ-H2Av foci, characteristic of DNA DSBs. Significantly, the ATR/Chk2 mutations do not suppress the defects in retrotransposon and *Stellate* silencing. We therefore conclude that rasiRNA-based gene silencing is not required for axis specification, and that the critical developmental function for the *Drosophila* rasiRNA pathway is to suppress DNA damage signaling in the germline.

Table 1. *mnk* and *mei-41* Mutations Suppress Dorsal-Ventral Patterning Defects in rasiRNA Mutants

	Dorsal Appendage (%) Phenotype				
Maternal Genotype	2 (Wild-Type)	1 (Fused)	0 (Absent)	Hatch Rate (%)	N
mnk^{p6}/mnk^{p6}	94.1	2.3	3.6	73.9	827
$mei\text{-}41^{D3}/mei\text{-}41^{D3}$	100	0	0	0	920
$mei\text{-}W68^{1}/mei\text{-}W68^{k05603}$	94.3	4	1.7	67.2	1281
$armi^{72.1}/armi^{1}$	3.5	67.6	28.9	0	765
mnk^{p6}/mnk^{p6}; $armi^{72.1}/armi^{1}$	91.9	2.5	5.6	0	1062
$mei\text{-}41^{D3}/mei\text{-}41^{D3}$; $armi^{72.1}/armi^{1}$	56	38.4	5.6	0	575
$mei\text{-}W68^{1}/mei\text{-}W68^{k05603}$; $armi^{72.1}/armi^{1}$	3.6	37.9	58.5	0	280
aub^{HN2}/aub^{QC42}	47.7	40.3	12	0	1212
mnk^{p6}, aub^{HN2}/mnk^{p6}, aub^{QC42}	97.6	2	0.4	0	296
$mei\text{-}41^{D3}/mei\text{-}41^{D3}$; aub^{HN2}/aub^{QC42}	85.2	8.6	6.2	0	859
$spn\text{-}E^{1}/spn\text{-}E^{1}$	16.6	55.4	27.9	0	123
$mei\text{-}41^{D3}/mei\text{-}41^{D3}$; $spn\text{-}E^{1}/spn\text{-}E^{1}$	23.9	56.2	19.9	0	233
$spn\text{-}D^{2}/spn\text{-}D^{2}$	34.8	54	11.2	17.3	1245
mnk^{p6}/mnk^{p6}; $spn\text{-}D^{2}/spn\text{-}D^{2}$	98.8	0.5	0.7	45.9	812

RESULTS

ATR and Chk2 Mutations Suppress *armi* and *aub* Axis Specification Defects

The *armi*, *spn-E*, and *aub* genes are required for production of rasiRNAs, and mutations in these genes lead to Stellate overexpression during spermatogenesis and premature Osk protein expression during oogenesis (Aravin et al., 2001; Cook et al., 2004; Vagin et al., 2006). These mutations also lead to female sterility and disrupt embryonic axis specification, suggesting that rasiRNAs control expression of genes involved in patterning the oocyte (Cook et al., 2004). However, mutations in the meiotic DSB repair pathway also lead to axis specification defects, and these defects result from activation of a damage-signaling pathway that includes the ATR and Chk2 kinases (Bartek et al., 2001; Abdu et al., 2002; Ghabrial and Schupbach, 1999). These findings raised the alternative possibility that rasiRNA pathway mutations disrupt axis specification by activating ATR and Chk2.

To genetically test the role of DNA damage signaling in the rasiRNA pathway mutant phenotype, we analyzed double-mutant combinations with *mei-41* or *mnk*, which encode the *Drosophila* ATR and Chk2 homologs, respectively. We were unable to recover *mnk; spn-E* double mutants, and it is unclear if this reflects a significant negative genetic interaction between these genes or the presence of background mutations on the *mnk* or *spn-E* chromosome. Our analyses thus focused on *armi* and *aub*, which we were able to combine with both *mei-41* and *mnk*. If *armi* and *aub* mutations block axis specification through ATR/Chk2 activation, the patterning defects associated with these mutations will be suppressed in the double mutants. Initial suppression analysis focused on the dorsal appendages, which are easily scored eggshell structures that are induced through Gurken (Grk) signaling from the oocyte to the somatic follicle cells during midoogenesis (Schupbach, 1987). Appendages do not form in the absence of Grk, a single appendage forms with low Grk levels, and two appendages form when signaling is normal (Gonzalez-Reyes et al., 1995; Roth et al., 1995). As shown in Table 1, *mei-41* and *mnk* dramatically suppress the appendage defects associated with *armi* and *aub*. Two appendages are present on 100% of the embryos derived from wild-type and *mei-41* females, and on 94% of the embryos derived from *mnk* single mutants (Table 1). By contrast, only 3.5% of the embryos derived from $armi^{72.1}/armi^{1}$ mutant females have two dorsal appendages. Strikingly, 92% of the embryos derived from *mnk;* $armi^{72.1}/armi^{1}$ double mutants show wild-type appendage morphology. Similarly, two appendages are present on 48% of the embryos derived from *aub* single mutants, and 98% of the embryos from *mnk, aub* double mutants have two appendages.

Mutations in *mei-41* also suppressed the eggshell patterning defects associated with *armi* and *aub*, although suppression by *mei-41* was consistently less dramatic than suppression by *mnk*. A total of 56% of the embryos from *mei-41;* $armi^{72.1}/armi^{1}$ double mutants show normal appendages. The *mei-41* mutation was also less effective than *mnk* in suppressing appendage defects associated with homozygous $armi^{1}$ (data not shown) and *aub* (Table 1). Therefore, partial suppression of the patterning defects by *mei-41* is not allele or gene specific. Chk2 can be activated by both ATR and ATM kinases (Bartek et al., 2001; Bartek and Lukas, 2003; Hirao et al., 2002), and the lower level of suppression by *mei-41*/ATR relative to *mnk*/Chk2 may therefore reflect redundant Chk2 activation by the

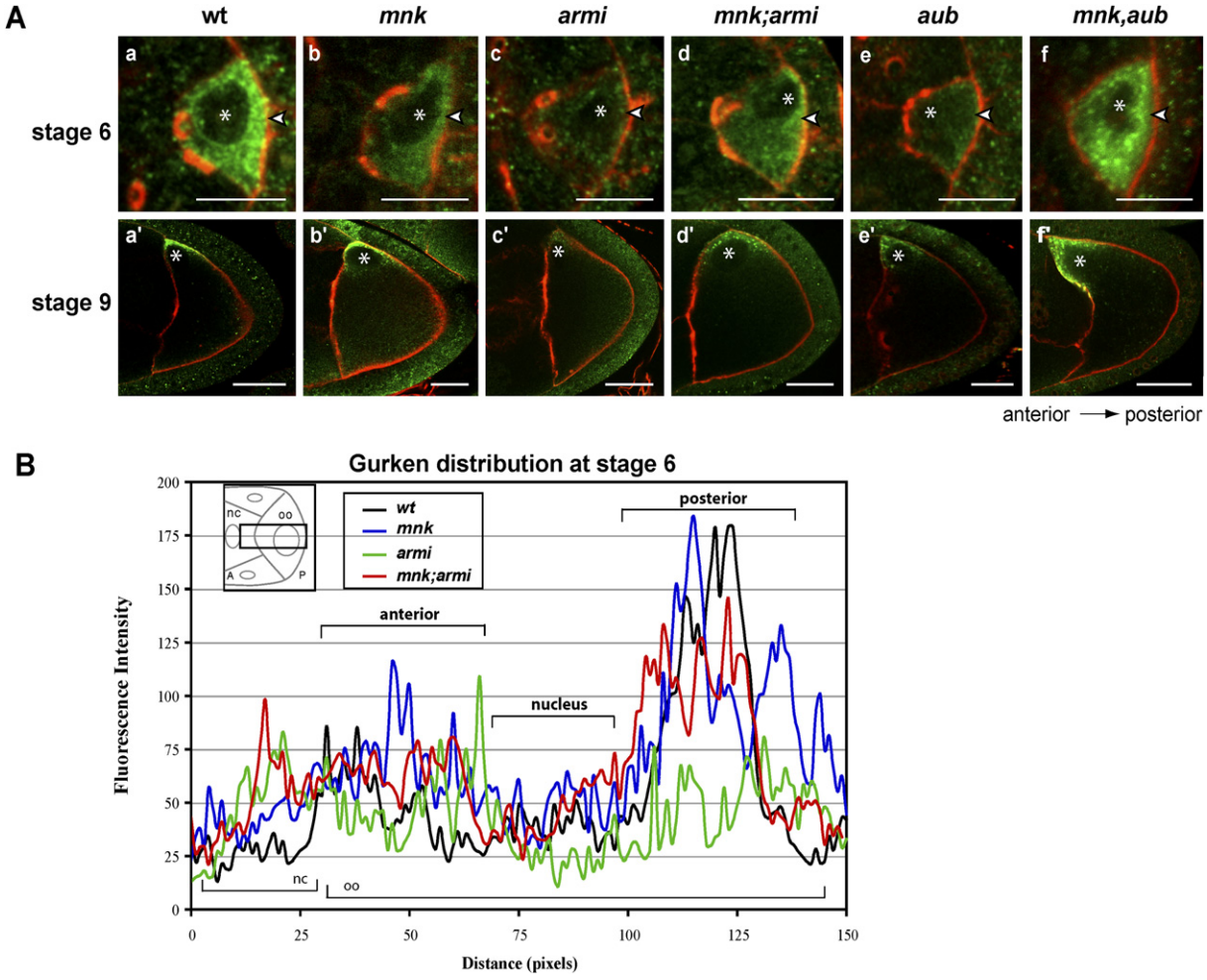

Figure 1. *mnk* Suppresses Gurken Protein Localization Defects in rasiRNA Mutants

(A) (a) In wild-type stage-6 egg chambers, Gurken (Grk) protein (green) accumulates at the posterior cortex (arrowhead). (a′) By stage 9, Grk is localized at the dorsal anterior cortex. Actin filaments (red) mark the cell boundaries. (b and b′) In mnk^{p6} oocytes, Grk localization is the same as in wild-type. (c and c′) In $armi^{72.1}/armi^{1}$ egg chambers, only low levels of Grk are present, and the protein is dispersed throughout the oocyte-nurse cell complex. (d and d′) Posterior and dorsal accumulation of Grk is restored in mnk^{p6}/mnk^{p6}; $armi^{72.1}/armi^{1}$ double mutants. (e) In aub^{QC42}/aub^{HN2} stage-6 egg chambers, Grk localization is similar to that of $armi^{72.1}/armi^{1}$ oocytes. (e′) At stage 9, Grk is localized correctly in aub^{QC42}/aub^{HN2}, but not at wild-type levels. (f and f′) In mnk^{p6}, aub^{QC42}/mnk^{p6}, aub^{HN2} egg chambers, the Grk localization level is restored. Images were acquired under identical conditions for either stage. Projections of three serial 0.6 μm optical sections are shown. The oocyte nucleus is indicated (asterisk). Scale bars are 10 μm and 25 μm for stage-6 and -9 egg chambers, respectively.

(B) Quantification of Grk localization in stage-6 oocytes. The average fluorescence intensity along a line beginning in the nurse cell cytoplasm and extending through a cross-section of the oocyte is shown (inset).

Drosophila ATM homolog. However, null alleles of the *Drosophila atm* gene are lethal (Oikemus et al., 2004), making direct tests of this hypothesis difficult. Nonetheless, these initial observations indicated that the axis specification defects associated with rasiRNA pathway mutations result from activation of an ATR/Chk2 kinase DNA damage signal.

The axis specification defects associated with repair mutations are suppressed by mutations in *mei-W68*, which encodes the *Drosophila* homolog of the Spo11 nuclease that catalyzes meiotic DSB formation (McKim and Hayashi-Hagihara, 1998). By contrast, *mei-W68* has no effect on the dorsal appendage defects associated with *armi* (Table 1). Meiotic breaks thus do not appear to be the source of damage in *armi* mutations.

Localization of Axis Specification Determinants

During early oogenesis, the TGFα homolog Grk localizes to the posterior of the oocyte and signals to the overlying follicle cells, inducing posterior differentiation. During mid-oogenesis, Grk signals from the oocyte to the dorsal follicle cells to generate the dorsal-ventral axis (Gonzalez-Reyes et al., 1995; Roth et al., 1995). Mutations in *armi* and *aub* disrupt Grk protein localization at both stages, leading to posterior and dorsal-ventral axis specification defects (Cook et al., 2004). To determine if the DNA

damage signaling mutations suppress the Grk localization defects in *armi* and *aub* mutants, we analyzed the distribution of this protein by indirect immunofluorescence and laser-scanning confocal microscopy (Figure 1). For these studies, Grk protein levels within cross-sections of stage-6 oocytes were measured, and an average fluorescence intensity profile for each genotype was generated (Figure 1B, inset). In wild-type stage-6 oocytes, Grk protein accumulates near the posterior cortex (Figure 1Aa). In *armi* and *aub* single mutants, by contrast, low levels of Grk protein are uniformly distributed in the oocyte and nurse cells (Figures 1Ac and 1Ae). However, Grk shows almost wild-type accumulation near the posterior cortex of *mnk; armi* and *mnk*, *aub* double mutant oocytes (Figures 1Ad and 1Af). The defects in dorsal-anterior localization of Grk during midoogenesis (Figures 1Ac′ and 1Ae′) are also restored in the *mnk* double mutants (Figures 1Ad′ and 1Af′). Weaker suppression is observed with *mei-41*, consistent with our analysis of the dorsal appendages (Figure S1; see the Supplemental Data available with this article online).

To determine if *mnk* and *mei-41* suppress the *armi*- and *aub*-induced defects in posterior morphogen localization (Cook et al., 2004), we analyzed the distribution of the pole plasm proteins Vasa (Vas) and Osk during midoogenesis. Osk localizes to the posterior in only 10% of stage-9 and -10 oocytes from *armi* females (2 of 23), and there is no detectable localization in the remaining egg chambers (Figure 2C). By contrast, Osk shows wild-type posterior accumulation in over 80% of stage-9 and -10 *mnk; armi* double mutants (27 of 33; Figure 2D). Vas localization to the posterior pole is similarly restored in the double mutants (not shown). *mei-41* leads to a less dramatic suppression of the posterior patterning defects (not shown). Osk and Vas localization is also disrupted in *aub* mutants (Figure 2E and data not shown), and localization is restored in double mutants with *mnk* and *mei-41* (Figure 2F). The defects in posterior and dorsal-ventral morphogen localization associated with both *armi* and *aub* thus require ATR and Chk2, which function in DNA damage signal transduction.

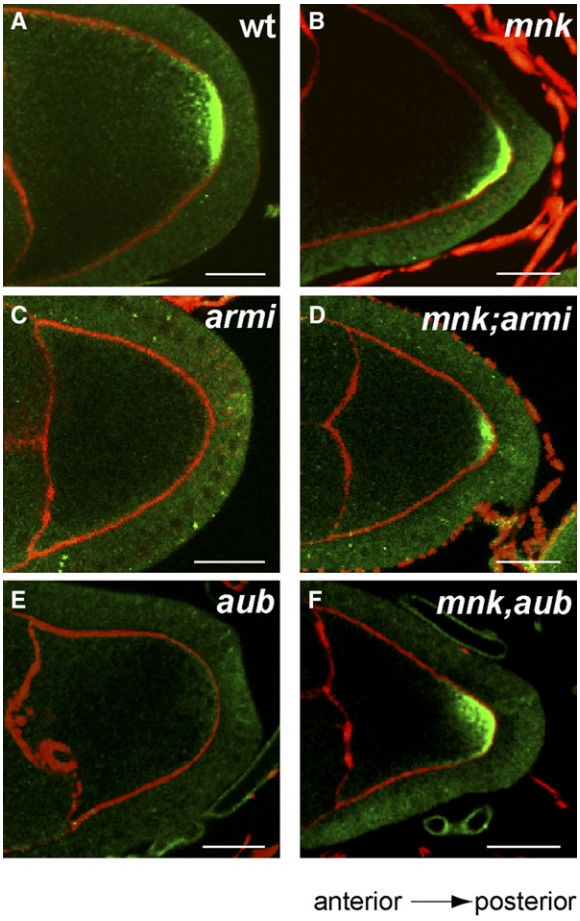

Figure 2. Oskar Protein Localization Defects Associated with rasiRNA Mutations Are Suppressed by *mnk*

(A–F) Egg chambers were fixed and labeled against Oskar (Osk) protein (green) and Actin (red). In stage-9 to -10 (A) wild-type and (B) mnk^{p6} mutant oocytes, Osk localizes tightly to the posterior cortex. In similarly staged (C) $armi^{72.1}/armi^{1}$ and (E) aub^{QC42}/aub^{HN2} oocytes, Osk fails to localize to the posterior pole. Osk localization is restored in the double mutants (D) mnk^{p6}; $armi^{72.1}/armi^{1}$ and (F) mnk^{p6}, aub^{QC42}/aub^{HN2}. Egg chambers are oriented with posterior to the right. Images were acquired under identical conditions. Single optical sections are shown. The scale bar is 20 μm.

Microtubule Organization and Vas Phosphorylation

Specification of the posterior pole is initiated during early oogenesis, when the microtubule cytoskeleton reorganizes to form a polarized scaffold in the oocyte-nurse cell complex. While these complexes are in the germarium, a prominent microtubule-organizing center (MTOC) forms at the anterior pole of the oocyte, and this MTOC appears to be required for oocyte differentiation (Figure 3Aa) (Theurkauf et al., 1993). After cysts bud from the germarium, a posterior MTOC is established (Figure 3Aa′). This asymmetric microtubule array directs Grk to the posterior pole of the oocyte, which signals to the overlying somatic follicle cells to induce posterior differentiation (Gonzalez-Reyes et al., 1995; Roth et al., 1995). In *armi* mutants, both the early anterior and later posterior MTOCs are much less prominent than in wild-type (Cook et al., 2004) (Figures 3Ab and 3Ab′; Figure S2). By contrast, egg chambers double mutant for *armi* and *mnk* show near-wild-type anterior and posterior MTOCs (Figures 3Ac and 3Ac′). Restoration of normal microtubule organization correlates with suppression of the Grk localization defects (Figure 1Ad). Egg chambers double mutant for *armi* and *mei-41* show a phenotype intermediate between the *armi* mutants and wild-type controls, consistent with partial suppression of posterior patterning defects later in oogenesis (Figure S2). The microtubule organization defects in *aub* are also strongly suppressed by *mnk*, and they are more weakly suppressed by *mei-41* (Figure S2). Mutations in *armi* and *aub* thus trigger Chk2-dependent defects in microtubule organization. These cytoskeletal defects are likely to contribute to the loss of axial patterning later in oogenesis.

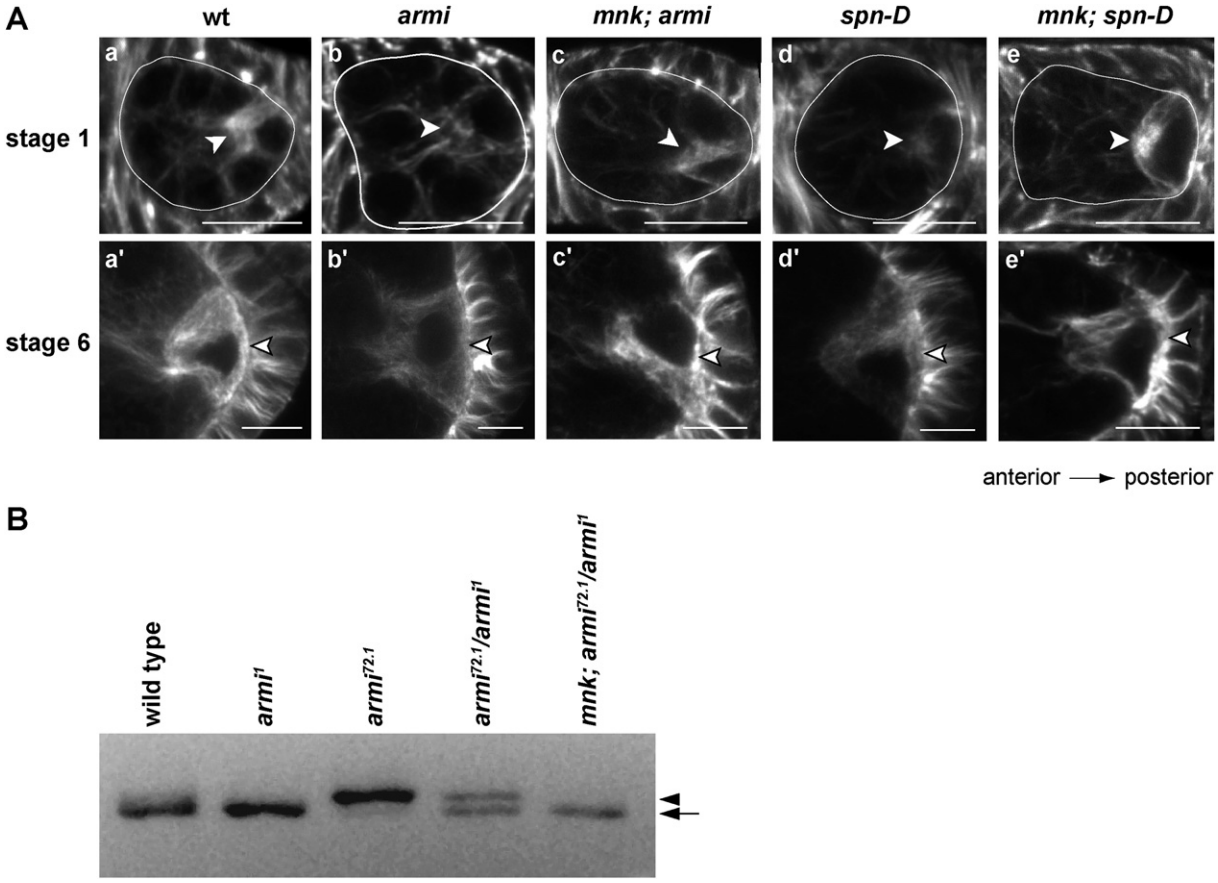

Figure 3. *mnk* Suppresses Microtubule Organization Defects and Vasa Phosphorylation in rasiRNA Pathway Mutants

(A) Microtubules were labeled with an anti-α-tubulin antibody. (a) A bright microtubule organizing center (MTOC) is localized to the anterior pole of the oocyte in wild-type stage-1 egg chambers (arrowhead). (a′) By stage 6, the MTOC is localized along the posterior cortex (arrowhead). In $armi^{72.1}/armi^{1}$ and $spn\text{-}D^{2}$ egg chambers, the (b and d) anterior MTOC and later (b′ and d′) posterior MTOC are much less prominent (arrowheads). (c and e) In mnk^{p6}; $armi^{72.1}/armi^{1}$ and mnk^{p6}; $spn\text{-}D^{2}$ egg chambers, (c and e) anterior MTOC during stage 1 (arrowheads) and the (c′ and e′) posterior MTOC during stage 6 (arrowheads) are restored. Stage-1 oocytes are outlined. Images were acquired under identical conditions. Projections of four serial 0.6 μm optical sections are shown. Posterior is oriented to the right. The scale bar is 10 μm.

(B) Western blot analysis of Vasa (Vas) protein in wild-type, $armi^{1}$, $armi^{72.1}$, $armi^{72.1}/armi^{1}$, and mnk^{p6}; $armi^{72.1}/armi^{1}$ ovary extracts. Vas from homozygous $armi^{72.1}$ ovaries has a reduced electrophoretic mobility relative to Vas from wild-type ovaries. Low-mobility and wild-type mobility forms of Vas are present in $armi^{72.1}/armi^{1}$ ovary extracts. Only the faster-migrating form is present in mnk^{p6}; $armi^{72.1}/armi^{1}$ extracts (arrow).

The axis specification defects associated with mutations that disrupt meiotic DSB repair are also suppressed by *mnk*. To determine if Chk2-dependent disruption of the oocyte cytoskeleton contributes to these defects, we analyzed microtubule organization in ovaries mutant for *spn-D*, which encodes a rad51C homolog required for DSB repair (Abdu et al., 2003). Mutations in *spn-D*, like mutations in *armi* and *aub*, disrupt both the prominent MTOC at the anterior of stage-1 egg chambers and the posterior MTOC during stages 2–6 (Figures 3Ad and 3Ad′). These defects are suppressed in *mnk; spn-D* double mutants (Figures 3Ae and 3Ae′), suggesting that DSB repair mutations and rasiRNA mutations trigger a common Chk2-dependent pathway that disrupts microtubule organization.

DSB repair mutations induce Chk2-dependent phosphorylation of Vas, a conserved RNA helicase required for posterior and dorsal-ventral patterning (Ghabrial and Schupbach, 1999; Styhler et al., 1998). To determine if rasiRNA mutations also trigger Chk2-dependent Vas phosphorylation, we probed western blots of *armi* and *mnk; armi* double mutants for Vas protein. Vas protein levels are also somewhat lower in the *armi* mutant egg chambers, but this may reflect differences in egg chamber-stage distribution in the isolated ovaries (Figure 3B). More significantly, a lower-electrophoretic mobility species is observed in ovaries homozygous for a strong loss-of-function allele, $armi^{72.1}$, and both species are observed with a weaker allelic combination, $armi^{72.1}/armi^{1}$. Only the faster-migrating species is present in *mnk;* $armi^{72.1}/armi^{1}$ double mutant extracts. After phosphatase treatment, the lower-mobility species present in *armi* mutant extracts disappears, and the faster-migrating species increases in intensity (not shown), indicating that the

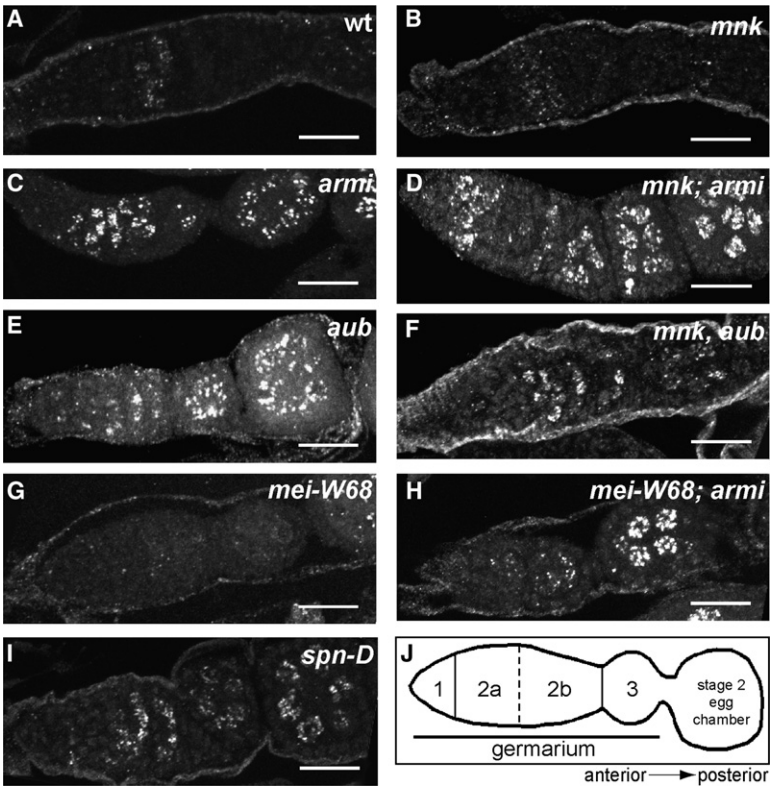

Figure 4. γ-H2Av Foci Accumulate in *armi* and *aub* Mutant Ovaries

(A–J) The phosphorylated form of histone H2Av (γ-H2Av) accumulates near double-strand break sites. (A and B) In wild-type and mnk^{p6} mutants, γ-H2Av foci are restricted to region 2 of the germarium, where meiotic DSBs form. (C–F) In (C) $armi^{72.1}/armi^{1}$, (D) $mnk^{p6}; armi^{72.1}/armi^{1}$, (E) aub^{QC42}/aub^{HN2}, and (F) mnk^{p6}, aub^{QC42}/mnk^{p6}, aub^{HN2} ovaries, γ-H2Av foci accumulate in germline cells within the germarium and persist and increase in intensity as cysts bud from the germarium to form egg chambers. (I) A similar pattern is observed in ovaries mutant for $spn\text{-}D^{2}$, which is required for DSB repair. (G) Mutations in *mei-W68* ($mei\text{-}W68^{1}/mei\text{-}W68^{k05603}$), which encodes the Spo11 nuclease that initiates meiotic DSBs, suppress formation of γ-H2Av foci in region 2 of the germarium. (H) However, *mei-W68* does not suppress γ-H2Av focus formation in *armi* mutants ($mei\text{-}W68^{1}/mei\text{-}W68^{k05603}; armi^{72.1}/armi^{1}$). (J) A schematic representation of the regions of the germarium and a developing egg chamber. Projections of six serial 1 μm optical sections are shown. Posterior is to the right. The scale bar is 20 μm.

lower-mobility band is a phosphorylated form of Vas. Mutations in *armi*, like meiotic DSB repair mutations, thus trigger Chk2-dependent phosphorylation of Vas. While the physiological significance of Vas phosphorylation has not been established, these findings support the hypothesis that *armi* mutations lead to Chk2 kinase activation.

rasiRNA Pathway Mutations Lead to Germline γ-H2Av Accumulation

The observations described above indicate that the axis specification defects associated with *armi* and *aub* are mediated by ATR and Chk2 kinases, which are normally activated by DNA DSBs. To determine if *armi* and *aub* lead to DSB accumulation, we labeled mutant ovaries for the phosphorylated form of the *Drosophila* histone H2AX variant (γ-H2Av), which accumulates on chromosomes near break sites (Modesti and Kanaar, 2001; Redon et al., 2002). After chromosome breakage, *Drosophila* H2Av, like H2AX, is phosphorylated at a conserved SQ motif within an extended C-terminal tail (Madigan et al., 2002; Rogakou et al., 1998). We therefore used an anti-phosphoprotein antibody specific for γ-H2Av (Gong et al., 2005). In wild-type ovaries, γ-H2Av foci are restricted to region 2 of the germarium, where meiotic DSBs are formed (Figure 4A) (Jang et al., 2003). Consistent with earlier observations, this labeling is significantly reduced in *mei-W68* mutants, which do not initiate meiotic breaks (Figure 4G). In *armi* and *aub* mutants, prominent γ-H2Av foci are present in germline cells of the germarium. Unlike wild-type, these foci persist and increase in intensity as cysts mature and bud to form stage-2 egg chambers (Figures 4C and 4E). γ-H2Av foci persist in double mutants with *mnk*, indicating that suppression of the patterning defects by *mnk* is not the result of enhanced DNA repair.

γ-H2Av foci also persist in egg chambers mutant for a third rasiRNA gene, *spn-E* (Figure S3). The pattern of germline-specific γ-H2Av accumulation in *armi*, *aub*, and *spn-E* is similar to the pattern of γ-H2Av accumulation in mutants for the DNA repair gene *spn-D*, although the foci appear to arise at somewhat earlier stages in the rasiRNA mutants (Figures 4C, 4E, and 4I). Accumulation of γ-H2Av foci in *spn-D* mutants is suppressed by *mei-W68*, consistent with a function for this gene in meiotic DSB repair (Abdu et al., 2002). By contrast, γ-H2Av foci persist in *mei-W68; armi* double mutants (Figure 4H). We have not yet assayed *mei-W68* double mutants with *aub* or *spn-E*, but the observation described above suggests that the γ-H2Av foci in rasiRNA pathway mutations are independent of meiotic DSB formation.

rasiRNA Function

The observations presented above strongly suggest that the axial patterning defects associated with *armi* and *aub* are a consequence of DNA damage signaling, and that rasiRNA-based gene silencing is not directly involved in embryonic patterning. However, the *mnk* and *mei-41* mutations could suppress the defects in rasiRNA function associated with *armi* and *aub*. We therefore analyzed

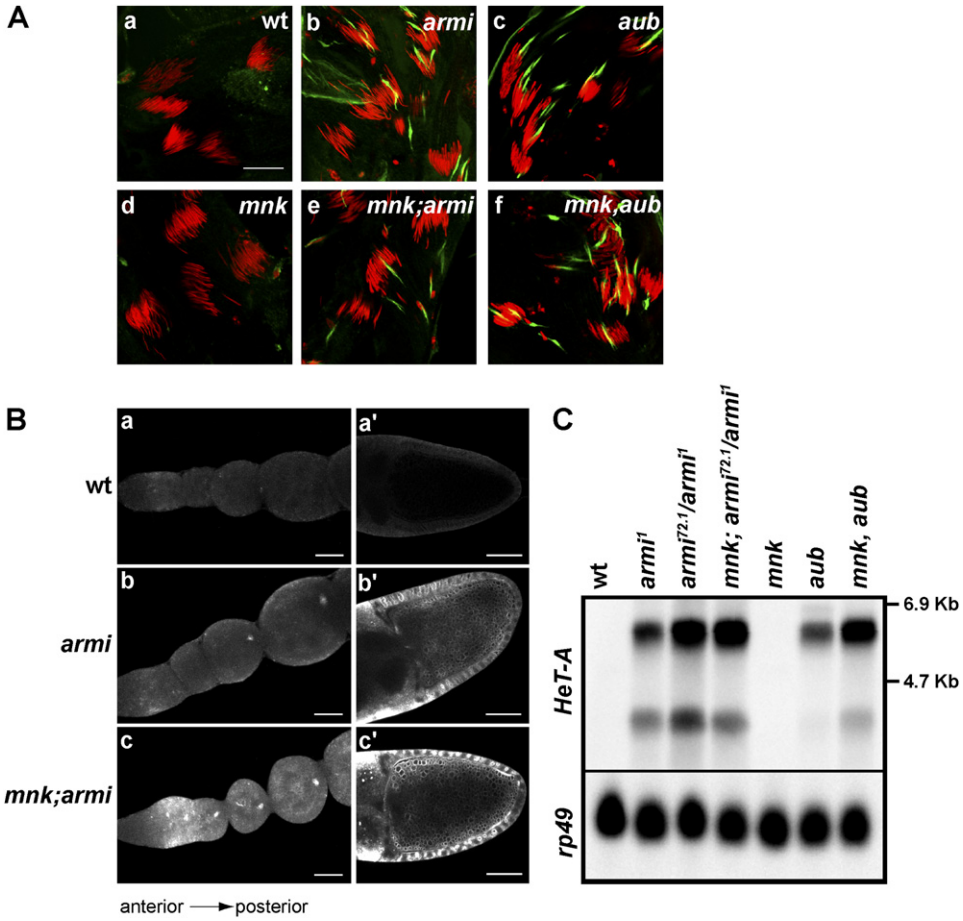

Figure 5. The *mnk* Mutation Does Not Suppress Defects in rasiRNA Function

(A) Silencing of the *Stellate* locus during spermatogenesis. *Stellate* is not expressed in (a) wild-type or (d) mnk^{p6} mutant testes. However, *Stellate* is overexpressed, and the protein assembles into crystals in testes from (b) $armi^{72.1}/armi^{1}$, (c) aub^{QC42}/aub^{HN2}, (e) mnk^{p6}; $armi^{72.1}/armi^{1}$, and (f) mnk^{p6}, aub^{QC42}/mnk^{p6}, aub^{HN2} males. DNA (red) was labeled with TOTO3, and Stellate protein (green) was detected with anti-Stellate antibody. Projections of five serial 1 μm optical sections are shown. The scale bar is 20 μm.

(B) FISH analysis of *HeT-A* retrotransposon silencing. (a and a′) In wild-type ovaries, only background levels of *HeT-A* expression are detected. (b–c′) By contrast, *HeT-A* is expressed at high levels in the germline and somatic follicle cells of early and midoogenesis-stage $armi^{72.1}/armi^{1}$ and mnk^{p6}; $armi^{72.1}/armi^{1}$ egg chambers. Panels (a), (b), and (c) are projections of 12–15 serial 1.5 μm optical sections. Panels (a′), (b′), and (c′) are single optical sections. Posterior is oriented to the right. The scale bar is 20 μm for the left panels and 50 μm for the right panels.

(C) Northern blot for *HeT-A*. Total ovary RNA samples were resolved on a 1% agarose/formaldehyde gel, transferred to membrane, and probed for the *HeT-A* transcript. *HeT-A* transcripts are undetectable in wild-type and mnk^{p6} samples, but they are abundant in RNA derived from $armi^{1}$, $armi^{72.1}/armi^{1}$, mnk^{p6}; $armi^{72.1}/armi^{1}$, aub^{QC42}/aub^{HN2}, and mnk^{p6}, aub^{QC42}/aub^{HN2} mutant ovaries. Ribosomal protein 49 (rp49) was used as a loading control.

rasiRNA-dependent silencing of both the *Stellate* gene during spermatogenesis and the *HeT-A* retrotransposon during oogenesis in single and double mutants. The *Stellate* gene is repressed during spermatogenesis, apparently through mRNA turnover guided by rasiRNAs derived from the *Suppressor of Stellate* locus (Aravin et al., 2001; Gvozdev et al., 2003). Mutations in *armi* and *aub* lead to accumulation of full-length *Stellate* mRNA and Stellate protein overexpression, which leads to the assembly of Stellate crystals in mutant testes (Aravin et al., 2004; Forstemann et al., 2005; Stapleton et al., 2001; Tomari et al., 2004a) (Figures 5Ab and 5Ac). Stellate crystals are present in both *mnk; armi* and *mnk, aub* double mutant testes (Figures 5Ae and 5Af). Stellate overexpression is also linked to male sterility, and *mnk; armi* males are also sterile (data not shown).

HeT-A is a retrotransposon that contributes to telomere formation in *Drosophila* (Pardue et al., 2005), and *HeT-A* expression is dramatically derepressed in *armi*, *aub*, and *spn-E* mutant ovaries (Aravin et al., 2001; Vagin et al., 2004, 2006). *HeT-A* is not expressed at detectable levels on northern blots of wild-type or *mnk* RNAs. However, *HeT-A* transcripts are abundant in *armi* and *aub* mutants (Figure 5C). Significantly, *HeT-A* is also overexpressed in *mnk; armi* and *mnk, aub* double mutants (Figures 5B and 5C). In fact, *HeT-A* expression is higher in the double mutants than in the single mutants. FISH analyses indicate that this reflects increased expression in the germline

and somatic cells of the ovary, during both early and mid-oogenesis (Figure 5B). Therefore, the *mnk* mutation does not suppress defects in rasiRNA-based gene silencing during spermatogenesis or oogenesis, leading us to conclude that rasiRNA-based silencing is not required for axis specification.

DISCUSSION

Mutations in the *Drosophila armi*, *aub*, and *spn-E* genes disrupt oocyte microtubule organization and asymmetric localization of mRNAs and proteins that specify the posterior pole and dorsal-ventral axis of the oocyte and embryo (Cook et al., 2004). Mutations in these genes block homology-dependent RNA cleavage and RISC assembly in ovary lysates (Tomari et al., 2004a), RNAi-based gene silencing during early embryogenesis (Kennerdell et al., 2002), rasiRNA production, and retrotransposon and *Stellate* silencing (Aravin et al., 2001; Vagin et al., 2006). Mutations in *dcr-2* and *ago-2* genes, by contrast, block siRNA function (Okamura et al., 2004; Tomari et al., 2004b), but they do not disrupt the rasiRNA pathway or embryonic axis specification (Vagin et al., 2006). The rasiRNA pathway thus appears to be required for embryonic axis specification. However, the function of rasiRNAs in the axis specification pathway has not been previously established.

Here, we show that the cytoskeletal polarization, morphogen localization, and eggshell patterning defects associated with *armi* and *aub* are efficiently suppressed by *mnk* and *mei-41*, which respectively encode Chk2 and ATR kinase components of the DNA damage signaling pathway (Figures 1–3; Table 1). In addition, we show that *armi* and *aub* mutants accumulate γ-H2Av foci characteristic of DNA DSBs (Figure 4) and trigger Chk2-dependent phosphorylation of Vas (Figure 3B), an RNA helicase required for posterior and dorsal-ventral specification (Styhler et al., 1998). Mutations in *spn-E* also disrupt the rasiRNA pathway (Aravin and Tuschl, 2005; Vagin et al., 2006), trigger axis specification defects (Cook et al., 2004), and lead to germline-specific accumulation of γ-H2Av foci (see Figure S3). Significantly, the *mnk* and *mei-41* mutations do not suppress Stellate or *HeT-A* overexpression, indicating that axis specification does not directly require rasiRNA-dependent gene silencing. Based on these findings, we conclude that the rasiRNA pathway suppresses DNA damage signaling in the female germline, and that mutations in this pathway disrupt axis specification by activating an ATR/Chk2 kinase pathway that blocks microtubule polarization and morphogen localization in the oocyte (Figure 6).

The cause of DNA damage signaling in *armi*, *aub*, and *spn-E* mutants remains to be established. In wild-type ovaries, γ-H2Av foci begin to accumulate in region 2 of the germarium (Jang et al., 2003), when the Spo11 nuclease (encoded by the *mei-W68* gene) initiates meiotic breaks (McKim and Hayashi-Hagihara, 1998). The axis specification defects associated with DNA DSB repair mutations are efficiently suppressed by *mei-W68* mutations, indicating that meiotic breaks are the source of

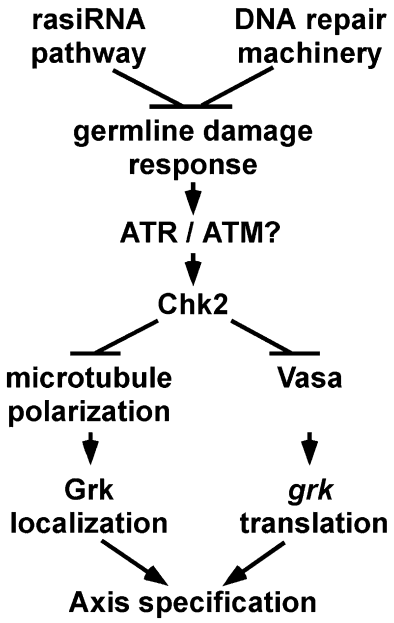

Figure 6. Model for rasiRNA Control of Axis Specification
The rasiRNA pathway and meiotic DSB repair machinery function independently to suppress DNA damage signaling in the female germline. Mutations that disrupt either pathway activate a common DNA damage response, mediated by the ATR and Chk2 kinases. Chk2 activation blocks axis specification by disrupting microtubule organization and phosphorylating Vas, an RNA helicase required for axis specification that has been implicated in *grk* mRNA translation.

DNA damage in these mutants (Abdu et al., 2002; Ghabrial and Schupbach, 1999; Staeva-Vieira et al., 2003). The axis specification defects and γ-H2Av focus formation associated with *armi*, by contrast, are not suppressed by *mei-W68* (Figure 4; Table 1). We have not yet analyzed *mei-W68* double mutants with *aub* or *spn-E*, but this observation strongly suggests that meiotic DSBs are not the source of DNA damage in rasiRNA pathway mutations. Retrotransposon silencing is disrupted in *armi*, *aub*, and *spn-E* mutants (Aravin et al., 2001; Vagin et al., 2006), and transcription of LINE retrotransposons in mammalian cells leads to DNA damage and DNA damage signaling (Belgnaoui et al., 2006; Gasior et al., 2006). Loss of retrotransposon silencing could therefore directly induce the DSBs in rasiRNA pathway mutants. However, DNA damage can also lead to loss of retrotransposon silencing (Bradshaw and McEntee, 1989; Farkash et al., 2006; Rudin and Thompson, 2001). Mutations in the rasiRNA pathway could therefore disrupt DNA repair and thus induce DNA damage, which, in turn, induces loss of retrotransposon silencing. Finally, the *HeT-A* retrotransposon is associated with telomeres, and overexpression of this element could reflect a loss of telomere protection and could damage signaling by chromosome ends in the rasiRNA pathway mutants. The available data do not distinguish between these alternatives.

In mouse, the *piwi*-related Argonauts Miwi and Mili bind piRNAs, 30 nt RNAs derived primarily from a single strand

that appear to be related to rasiRNAs (Aravin et al., 2006; Girard et al., 2006; Grivna et al., 2006). Mutations in these genes disrupt spermatogenesis and lead to germline apoptosis (Deng and Lin, 2002; Kuramochi-Miyagawa et al., 2001), which can be induced by DNA damage signaling. Mammalian piRNAs and *Drosophila* rasiRNAs may therefore serve similar functions in suppressing a germline-specific DNA damage response.

EXPERIMENTAL PROCEDURES

Drosophila Stocks

All animals were raised at 25°C on standard food. *Oregon R* was used for wild-type control. The following alleles were used: mnk^{p6} (Brodsky et al., 2004; Takada et al., 2003); $armi^{72.1}$ and $armi^{1}$ (Cook et al., 2004); $mei\text{-}41^{D3}$ (Hari et al., 1995; Hawley and Tartof, 1983); aub^{QC42}, aub^{HN2} (Schupbach and Wieschaus, 1991); $spn\text{-}E^{1}$ (Gillespie and Berg, 1995; Gonzalez-Reyes et al., 1997); $spn\text{-}D^{2}$ (Abdu et al., 2003); and P[*lacW*]-$mei\text{-}W68^{k05603}$, $mei\text{-}W68^{1}$ (McKim and Hayashi-Hagihara, 1998). The mnk^{p6} allele was kindly provided by M. Brodsky (Brodsky et al., 2004). All other stocks were obtained from the Bloomington *Drosophila* Stock Center (Drysdale et al., 2005; http://flybase.org/). Standard genetic procedures were used to generate double mutant combinations.

Antibody Production

Primers annealing to each of the translation start and stop sites of a *Stellate* cDNA (Bozzetti et al., 1995) were designed (Integrated DNA Technologies, Inc.) with attached Gateway (Invitrogen) sequences. The resulting PCR product was used to make a DONR clone, which, in turn, was used to subclone into the 6X-His-tagged Gateway vector pDest17, yielding a 29 kDa 6X-His-tagged Stellate fusion protein. The fusion protein was purified on a Probond Ni matrix (Invitrogen) under denaturing conditions, isolated by SDS-PAGE, and used to immunize two rabbits (Pocono Rabbit Farm and Laboratory, Inc.) by following standard protocols for antibody production. Antiserum was used at 1:1000 for immunohistochemistry.

Immunohistochemistry

Egg chamber fixation and whole-mount antibody labeling were performed as previously described (Theurkauf, 1994). Microtubules were labeled with FITC-conjugated mouse monoclonal anti-α-tubulin (Sigma Chemical Co.) used at 1:200. Osk protein was labeled with rabbit polyclonal anti-Osk antibody (Vanzo and Ephrussi, 2002) at 1:1000. Vas protein was labeled with rabbit polyclonal anti-Vas antibody (Liang et al., 1994) at 1:1000. Grk protein was labeled with mouse monoclonal anti-Grk antibody (obtained from the Developmental Studies Hybridoma Bank, University of Iowa) at 1:10. Antibody against γ-H2Av was kindly provided by Kim McKim (Gong et al., 2005), and egg chambers were labeled as described previously (Belmont et al., 1989). Rhodamine-conjugated phalloidin (Molecular Probes) was used at 1:100 to stain F-actin, and TOTO3 (Molecular Probes) was used at 1:500 (0.2 μM final concentration) to visualize DNA.

Fluorescence In Situ Hybridization

An antisense *HeT-A* digoxygenin (DIG)-labeled RNA probe was synthesized in vitro from a 500 bp PCR-amplified cDNA fragment carrying a T7 promoter (generously provided by P. Zamore) with a DIG RNA Labeling Kit by following the manufacturer's instructions (Roche). Whole-mount in situ hybridization was performed as described previously (Tautz, 1988; Tautz and Pfeifle, 1989; Cha et al., 2001). Tyramide signal amplification (TSA) was performed by following the manufacturer's instructions (Perkin Elmer).

Northern Blots

Fly ovaries were dissected in 1× Robb's medium (55 mM potassium acetate, 40 mM sodium acetate, 100 mM sucrose, 10 mM glucose, 1.2 mM $MgCl_2$, 1 mM $CaCl_2$, and 100 mM HEPES [pH 7.4]). Total RNA was isolated from ~30 mg ovaries by using the RNeasy Mini Kit by following the manufacturer's instructions (Qiagen). Approximately 20 μg total RNA/sample was resolved electrophoretically on a 1% agarose/formaldehyde gel. RNA was transferred to a positively charged nylon membrane (Roche) by standard capillary transfer. After transfer, RNA was fixed to the membrane via UV crosslinking (Stratalinker UV Crosslinker 2400). After prehybridization, blots were probed with DIG-labeled RNA by following the manufacturer's recommendations (Roche). *rp49* was used as a loading control. Blots were developed with CDP-Star (Tropix) according to the manufacturer's directions. Images were acquired with the Kodak 4000MM Image Station.

Western Blot Analysis

The western blot was performed as described (Ghabrial et al., 1998; Ghabrial and Schupbach, 1999); the rabbit polyclonal anti-Vas antibody was used at 1:5000.

Microscopy

All tissues were mounted in 90% glycerol/PBS, with 1 mg/ml p-Phenylenediamine (Sigma). Samples were analyzed with a Leica TCS-SP inverted laser-scanning microscope with 63× NA 1.32 PlanApo oil and 40× NA 1.25 Planapo oil objectives. Identical imaging conditions were used for each set of wild-type and mutant samples. Images were processed with Image J software.

Supplemental Data

Supplemental Data include three figures and are available at http://www.developmentalcell.com/cgi/content/full/12/1/45/DC1/.

ACKNOWLEDGMENTS

We thank Kim McKim and Anne Ephrussi for antibodies, and Alla Sigova, Vasia Vagin, and Phil Zamore for the *HeT-A* PCR probe. We also thank Beatrice Benoit and Hanne Varmark for helpful comments on the manuscript; Phil Zamore, Vasia Vagin, Klaus Forstemann, and Yuki Tomari for stimulating discussion and for sharing data prior to publication; and Beatrice Benoit for technical support. The Grk monoclonal antibody 1D12 was obtained from the Developmental Studies Hybridoma Bank developed under the auspices of the National Institute of Child Health and Human Development (NICHD) and maintained by the University of Iowa, Department of Biological Sciences. This work was supported by a grant to W.E.T. from the NICHD, National Institutes of Health (R01 HD049116).

Received: June 30, 2006
Revised: November 10, 2006
Accepted: December 2, 2006
Published: January 8, 2007

REFERENCES

Abdu, U., Brodsky, M., and Schupbach, T. (2002). Activation of a meiotic checkpoint during *Drosophila* oogenesis regulates the translation of Gurken through Chk2/Mnk. Curr. Biol. *12*, 1645–1651.

Abdu, U., Gonzalez-Reyes, A., Ghabrial, A., and Schupbach, T. (2003). The *Drosophila* spn-D gene encodes a RAD51C-like protein that is required exclusively during meiosis. Genetics *165*, 197–204.

Aravin, A., and Tuschl, T. (2005). Identification and characterization of small RNAs involved in RNA silencing. FEBS Lett. *579*, 5830–5840.

Aravin, A., Gaidatzis, D., Pfeffer, S., Lagos-Quintana, M., Landgraf, P., Iovino, N., Morris, P., Brownstein, M.J., Kuramochi-Miyagawa, S., Nakano, T., et al. (2006). A novel class of small RNAs bind to MILI protein in mouse testes. Nature *442*, 203–207.

Aravin, A.A., Naumova, N.M., Tulin, A.V., Vagin, V.V., Rozovsky, Y.M., and Gvozdev, V.A. (2001). Double-stranded RNA-mediated silencing

of genomic tandem repeats and transposable elements in the *D. melanogaster* germline. Curr. Biol. *11*, 1017–1027.

Aravin, A.A., Klenov, M.S., Vagin, V.V., Bantignies, F., Cavalli, G., and Gvozdev, V.A. (2004). Dissection of a natural RNA silencing process in the *Drosophila* melanogaster germ line. Mol. Cell. Biol. *24*, 6742–6750.

Bartek, J., and Lukas, J. (2003). Chk1 and Chk2 kinases in checkpoint control and cancer. Cancer Cell *3*, 421–429.

Bartek, J., Falck, J., and Lukas, J. (2001). CHK2 kinase–a busy messenger. Nat. Rev. Mol. Cell Biol. *2*, 877–886.

Belgnaoui, S.M., Gosden, R.G., Semmes, O.J., and Haoudi, A. (2006). Human LINE-1 retrotransposon induces DNA damage and apoptosis in cancer cells. Cancer Cell Int. *6*, 13.

Belmont, A.S., Braunfeld, M.B., Sedat, J.W., and Agard, D.A. (1989). Large-scale chromatin structural domains within mitotic and interphase chromosomes in vivo and in vitro. Chromosoma *98*, 129–143.

Bernstein, E., Kim, S.Y., Carmell, M.A., Murchison, E.P., Alcorn, H., Li, M.Z., Mills, A.A., Elledge, S.J., Anderson, K.V., and Hannon, G.J. (2003). Dicer is essential for mouse development. Nat. Genet. *35*, 215–217.

Bozzetti, M.P., Massari, S., Finelli, P., Meggio, F., Pinna, L.A., Boldyreff, B., Issinger, O.G., Palumbo, G., Ciriaco, C., Bonaccorsi, S., et al. (1995). The Ste locus, a component of the parasitic cry-Ste system of *Drosophila melanogaster*, encodes a protein that forms crystals in primary spermatocytes and mimics properties of the β subunit of casein kinase 2. Proc. Natl. Acad. Sci. USA *92*, 6067–6071.

Bradshaw, V.A., and McEntee, K. (1989). DNA damage activates transcription and transposition of yeast Ty retrotransposons. Mol. Gen. Genet. *218*, 465–474.

Brodsky, M.H., Weinert, B.T., Tsang, G., Rong, Y.S., McGinnis, N.M., Golic, K.G., Rio, D.C., and Rubin, G.M. (2004). *Drosophila melanogaster* MNK/Chk2 and p53 regulate multiple DNA repair and apoptotic pathways following DNA damage. Mol. Cell. Biol. *24*, 1219–1231.

Cha, B.J., Koppetsch, B.S., and Theurkauf, W.E. (2001). In vivo analysis of *Drosophila* bicoid mRNA localization reveals a novel microtubule-dependent axis specification pathway. Cell *106*, 35–46.

Cook, H., Koppetsch, B., Wu, J., and Theurkauf, W. (2004). The *Drosophila* SDE3 homolog *armitage* is required for oskar mRNA silencing and embryonic axis specification. Cell *116*, 817–829.

Deng, W., and Lin, H. (2002). miwi, a murine homolog of piwi, encodes a cytoplasmic protein essential for spermatogenesis. Dev. Cell *2*, 819–830.

Deshpande, G., Calhoun, G., and Schedl, P. (2005). *Drosophila argonaute-2* is required early in embryogenesis for the assembly of centric/centromeric heterochromatin, nuclear division, nuclear migration, and germ-cell formation. Genes Dev. *19*, 1680–1685.

Drysdale, R.A., Crosby, M.A., and The FlyBase Consortium (2005). Flybase: genes and gene models. Nucleic Acids Res. *33*, D390–D395.

Farkash, E.A., Kao, G.D., Horman, S.R., and Prak, E.T. (2006). Gamma radiation increases endonuclease-dependent L1 retrotransposition in a cultured cell assay. Nucleic Acids Res. *34*, 1196–1204.

Forstemann, K., Tomari, Y., Du, T., Vagin, V.V., Denli, A.M., Bratu, D.P., Klattenhoff, C., Theurkauf, W.E., and Zamore, P.D. (2005). Normal microRNA maturation and germ-line stem cell maintenance requires Loquacious, a double-stranded RNA-binding domain protein. PLoS Biol. *3*, e236.

Fukagawa, T., Nogami, M., Yoshikawa, M., Ikeno, M., Okazaki, T., Takami, Y., Nakayama, T., and Oshimura, M. (2004). Dicer is essential for formation of the heterochromatin structure in vertebrate cells. Nat. Cell Biol. *6*, 784–791.

Galiana-Arnoux, D., Dostert, C., Schneemann, A., Hoffmann, J.A., and Imler, J.L. (2006). Essential function in vivo for Dicer-2 in host defense against RNA viruses in *Drosophila*. Nat. Immunol. *7*, 590–597.

Gasior, S.L., Wakeman, T.P., Xu, B., and Deininger, P.L. (2006). The human LINE-1 retrotransposon creates DNA double-strand breaks. J. Mol. Biol. *357*, 1383–1393.

Ghabrial, A., and Schupbach, T. (1999). Activation of a meiotic checkpoint regulates translation of Gurken during *Drosophila* oogenesis. Nat. Cell Biol. *1*, 354–357.

Ghabrial, A., Ray, R.P., and Schupbach, T. (1998). okra and spindle-B encode components of the RAD52 DNA repair pathway and affect meiosis and patterning in *Drosophila* oogenesis. Genes Dev. *12*, 2711–2723.

Gillespie, D.E., and Berg, C.A. (1995). Homeless is required for RNA localization in *Drosophila* oogenesis and encodes a new member of the DE-H family of RNA-dependent ATPases. Genes Dev. *9*, 2495–2508.

Giraldez, A.J., Cinalli, R.M., Glasner, M.E., Enright, A.J., Thomson, J.M., Baskerville, S., Hammond, S.M., Bartel, D.P., and Schier, A.F. (2005). MicroRNAs regulate brain morphogenesis in zebrafish. Science *308*, 833–838.

Girard, A., Sachidanandam, R., Hannon, G.J., and Carmell, M.A. (2006). A germline-specific class of small RNAs binds mammalian Piwi proteins. Nature *442*, 199–202.

Gong, W.J., McKim, K.S., and Hawley, R.S. (2005). All paired up with no place to go: pairing, synapsis, and DSB formation in a balancer heterozygote. PLoS Genet. *1*, e67.

Gonzalez-Reyes, A., Elliott, H., and St Johnston, D. (1995). Polarization of both major body axes in *Drosophila* by gurken-torpedo signalling. Nature *375*, 654–658.

Gonzalez-Reyes, A., Elliott, H., and St Johnston, D. (1997). Oocyte determination and the origin of polarity in *Drosophila*: the role of the spindle genes. Development *124*, 4927–4937.

Grishok, A., Pasquinelli, A.E., Conte, D., Li, N., Parrish, S., Ha, I., Baillie, D.L., Fire, A., Ruvkun, G., and Mello, C.C. (2001). Genes and mechanisms related to RNA interference regulate expression of the small temporal RNAs that control *C. elegans* developmental timing. Cell *106*, 23–34.

Grivna, S.T., Beyret, E., Wang, Z., and Lin, H. (2006). A novel class of small RNAs in mouse spermatogenic cells. Genes Dev. *20*, 1709–1714.

Gvozdev, V.A., Aravin, A.A., Abramov, Y.A., Klenov, M.S., Kogan, G.L., Lavrov, S.A., Naumova, N.M., Olenkina, O.M., Tulin, A.V., and Vagin, V.V. (2003). Stellate repeats: targets of silencing and modules causing cis-inactivation and trans-activation. Genetica *117*, 239–245.

Hannon, G.J. (2002). RNA interference. Nature *418*, 244–251.

Hari, K.L., Santerre, A., Sekelsky, J.J., McKim, K.S., Boyd, J.B., and Hawley, R.S. (1995). The mei-41 gene of *D. melanogaster* is a structural and functional homolog of the human ataxia telangiectasia gene. Cell *82*, 815–821.

Hatfield, S.D., Shcherbata, H.R., Fischer, K.A., Nakahara, K., Carthew, R.W., and Ruohola-Baker, H. (2005). Stem cell division is regulated by the microRNA pathway. Nature *435*, 974–978.

Hawley, R.S., and Tartof, K.D. (1983). The effect of mei-41 on rDNA redundancy in *Drosophila melanogaster*. Genetics *104*, 63–80.

Hirao, A., Cheung, A., Duncan, G., Girard, P.M., Elia, A.J., Wakeham, A., Okada, H., Sarkissian, T., Wong, J.A., Sakai, T., et al. (2002). Chk2 is a tumor suppressor that regulates apoptosis in both an ataxia telangiectasia mutated (ATM)-dependent and an ATM-independent manner. Mol. Cell. Biol. *22*, 6521–6532.

Hutvagner, G., and Zamore, P.D. (2002). A microRNA in a multiple-turnover RNAi enzyme complex. Science *297*, 2056–2060.

Jang, J.K., Sherizen, D.E., Bhagat, R., Manheim, E.A., and McKim, K.S. (2003). Relationship of DNA double-strand breaks to synapsis in *Drosophila*. J. Cell Sci. *116*, 3069–3077.

Kennerdell, J.R., Yamaguchi, S., and Carthew, R.W. (2002). RNAi is activated during *Drosophila* oocyte maturation in a manner dependent on *aubergine* and *spindle-E*. Genes Dev. *16*, 1884–1889.

Kuramochi-Miyagawa, S., Kimura, T., Yomogida, K., Kuroiwa, A., Tadokoro, Y., Fujita, Y., Sato, M., Matsuda, Y., and Nakano, T. (2001). Two mouse piwi-related genes: miwi and mili. Mech. Dev. *108*, 121–133.

Lee, Y.S., Nakahara, K., Pham, J.W., Kim, K., He, Z., Sontheimer, E.J., and Carthew, R.W. (2004). Distinct roles for *Drosophila* Dicer-1 and Dicer-2 in the siRNA/miRNA silencing pathways. Cell *117*, 69–81.

Liang, L., Diehl-Jones, W., and Lasko, P. (1994). Localization of Vasa protein to the *Drosophila* pole plasm is independent of its RNA-binding and helicase activities. Development *120*, 1201–1211.

Madigan, J.P., Chotkowski, H.L., and Glaser, R.L. (2002). DNA double-strand break-induced phosphorylation of *Drosophila* histone variant H2Av helps prevent radiation-induced apoptosis. Nucleic Acids Res. *30*, 3698–3705.

McKim, K.S., and Hayashi-Hagihara, A. (1998). mei-W68 in *Drosophila melanogaster* encodes a Spo11 homolog: evidence that the mechanism for initiating meiotic recombination is conserved. Genes Dev. *12*, 2932–2942.

Modesti, M., and Kanaar, R. (2001). DNA repair: spot(light)s on chromatin. Curr. Biol. *11*, R229–R232.

Oikemus, S.R., McGinnis, N., Queiroz-Machado, J., Tukachinsky, H., Takada, S., Sunkel, C.E., and Brodsky, M.H. (2004). *Drosophila* atm/telomere fusion is required for telomeric localization of HP1 and telomere position effect. Genes Dev. *18*, 1850–1861.

Okamura, K., Ishizuka, A., Siomi, H., and Siomi, M.C. (2004). Distinct roles for Argonaute proteins in small RNA-directed RNA cleavage pathways. Genes Dev. *18*, 1655–1666.

Pardue, M.L., Rashkova, S., Casacuberta, E., DeBaryshe, P.G., George, J.A., and Traverse, K.L. (2005). Two retrotransposons maintain telomeres in *Drosophila*. Chromosome Res. *13*, 443–453.

Provost, P., Silverstein, R.A., Dishart, D., Walfridsson, J., Djupedal, I., Kniola, B., Wright, A., Samuelsson, B., Radmark, O., and Ekwall, K. (2002). Dicer is required for chromosome segregation and gene silencing in fission yeast cells. Proc. Natl. Acad. Sci. USA *99*, 16648–16653.

Redon, C., Pilch, D., Rogakou, E., Sedelnikova, O., Newrock, K., and Bonner, W. (2002). Histone H2A variants H2AX and H2AZ. Curr. Opin. Genet. Dev. *12*, 162–169.

Rogakou, E.P., Pilch, D.R., Orr, A.H., Ivanova, V.S., and Bonner, W.M. (1998). DNA double-stranded breaks induce histone H2AX phosphorylation on serine 139. J. Biol. Chem. *273*, 5858–5868.

Roth, S., Neuman-Silberberg, F.S., Barcelo, G., and Schupbach, T. (1995). cornichon and the EGF receptor signaling process are necessary for both anterior-posterior and dorsal-ventral pattern formation in *Drosophila*. Cell *81*, 967–978.

Rudin, C.M., and Thompson, C.B. (2001). Transcriptional activation of short interspersed elements by DNA-damaging agents. Genes Chromosomes Cancer *30*, 64–71.

Schupbach, T. (1987). Germ line and soma cooperate during oogenesis to establish the dorsoventral pattern of egg shell and embryo in *Drosophila melanogaster*. Cell *49*, 699–707.

Schupbach, T., and Wieschaus, E. (1991). Female sterile mutations on the second chromosome of *Drosophila melanogaster*. II. Mutations blocking oogenesis or altering egg morphology. Genetics *129*, 1119–1136.

Staeva-Vieira, E., Yoo, S., and Lehmann, R. (2003). An essential role of DmRad51/SpnA in DNA repair and meiotic checkpoint control. EMBO J. *22*, 5863–5874.

Stapleton, W., Das, S., and McKee, B.D. (2001). A role of the *Drosophila* homeless gene in repression of Stellate in male meiosis. Chromosoma *110*, 228–240.

Styhler, S., Nakamura, A., Swan, A., Suter, B., and Lasko, P. (1998). vasa is required for GURKEN accumulation in the oocyte, and is involved in oocyte differentiation and germline cyst development. Development *125*, 1569–1578.

Takada, S., Kelkar, A., and Theurkauf, W.E. (2003). *Drosophila* checkpoint kinase 2 couples centrosome function and spindle assembly to genomic integrity. Cell *113*, 87–99.

Tautz, D. (1988). Regulation of the *Drosophila* segmentation gene hunchback by two maternal morphogenetic centres. Nature *332*, 281–284.

Tautz, D., and Pfeifle, C. (1989). A non-radioactive in situ hybridization method for the localization of specific RNAs in *Drosophila* embryos reveals translational control of the segmentation gene hunchback. Chromosoma *98*, 81–85.

Theurkauf, W.E. (1994). Immunofluorescence analysis of the cytoskeleton during oogenesis and early embryogenesis. Methods Cell Biol. *44*, 489–505.

Theurkauf, W.E., Alberts, B.M., Jan, Y.N., and Jongens, T.A. (1993). A central role for microtubules in the differentiation of *Drosophila* oocytes. Development *118*, 1169–1180.

Tomari, Y., Du, T., Haley, B., Schwarz, D., Bennett, R., Cook, H., Koppetsch, B., Theurkauf, W., and Zamore, P.D. (2004a). RISC assembly defects in the *Drosophila* RNAi mutant *armitage*. Cell *116*, 831–841.

Tomari, Y., Matranga, C., Haley, B., Martinez, N., and Zamore, P.D. (2004b). A protein sensor for siRNA asymmetry. Science *306*, 1377–1380.

Vagin, V.V., Klenov, M.S., Kalmykova, A., Stolyarenko, A.D., Kotelnikov, R.N., and Gvozdev, V. (2004). The RNA interference proteins and vasa locus are involved in the silencing of retrotransposons in the female germline of *Drososophla melanogaster*. RNA Biology *1*, 54–58.

Vagin, V.V., Sigova, A., Li, C., Seitz, H., Gvozdev, V., and Zamore, P.D. (2006). A small RNA mechanism distinct from the RNAi and microRNA pathways silences selfish genetic elements in *Drosophila*. Science *313*, 320–324.

Vanzo, N.F., and Ephrussi, A. (2002). Oskar anchoring restricts pole plasm formation to the posterior of the *Drosophila* oocyte. Development *129*, 3705–3714.

Volpe, T., Schramke, V., Hamilton, G.L., White, S.A., Teng, G., Martienssen, R.A., and Allshire, R.C. (2003). RNA interference is required for normal centromere function in fission yeast. Chromosome Res. *11*, 137–146.

Wang, X.H., Aliyari, R., Li, W.X., Li, H.W., Kim, K., Carthew, R., Atkinson, P., and Ding, S.W. (2006). RNA interference directs innate immunity against viruses in adult *Drosophila*. Science *312*, 452–454.

Wassenegger, M. (2005). The role of the RNAi machinery in heterochromatin formation. Cell *122*, 13–16.